

Supplementary materials for “Control of Multiferroic properties in BiFeO₃ nanoparticles”

Diego Carranza-Celis¹, Alexander Cardona Rodríguez¹, Jackeline Narváez¹, Oscar Moscoso^{2,3}, Diego Muraca², Marcelo Knobel², Nancy Ornelas-Soto⁴, Andreas Reiber⁵, Juan Gabriel Ramírez¹,

¹*Department of Physics, Universidad de los Andes, Bogotá 111711, Colombia*

²*Instituto de Física ‘Gleb Wataghin’, Universidade Estadual de Campinas (UNICAMP), CEP13083-859 Campinas, São Paulo, Brazil*

³*Facultad de Ingeniería, Universidad Autónoma de Manizales, Manizales, Colombia*

⁴*Tecnologico de Monterrey, Escuela de Ingeniería y Ciencias, Ave. Eugenio Garza Sada 2501, 64849 Monterrey, N.L., México*

⁵*Department of Chemistry, Universidad de los Andes, Bogotá 111711, Colombia*

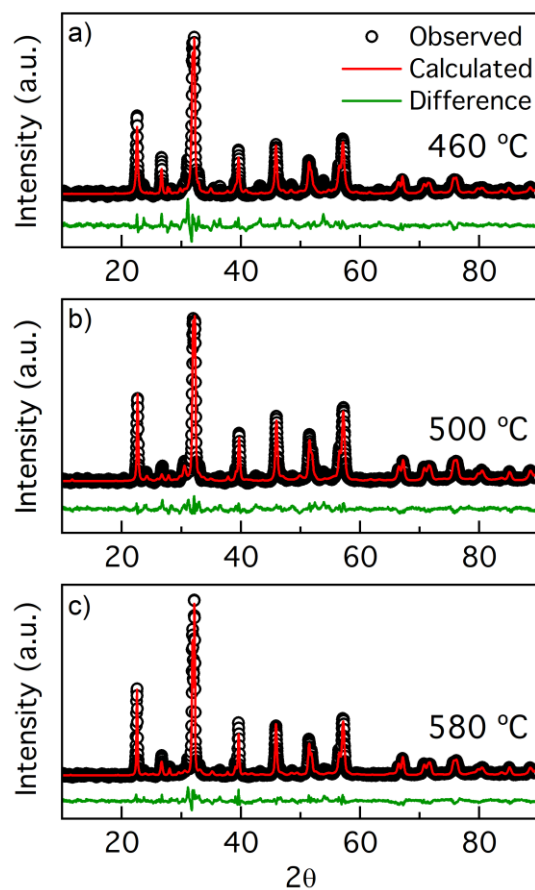


Figure S1. X-ray diffractograms and Rietveld refinement for NPs calcined at (a) 460 °C, (b) 500 °C and (d) 580 °C

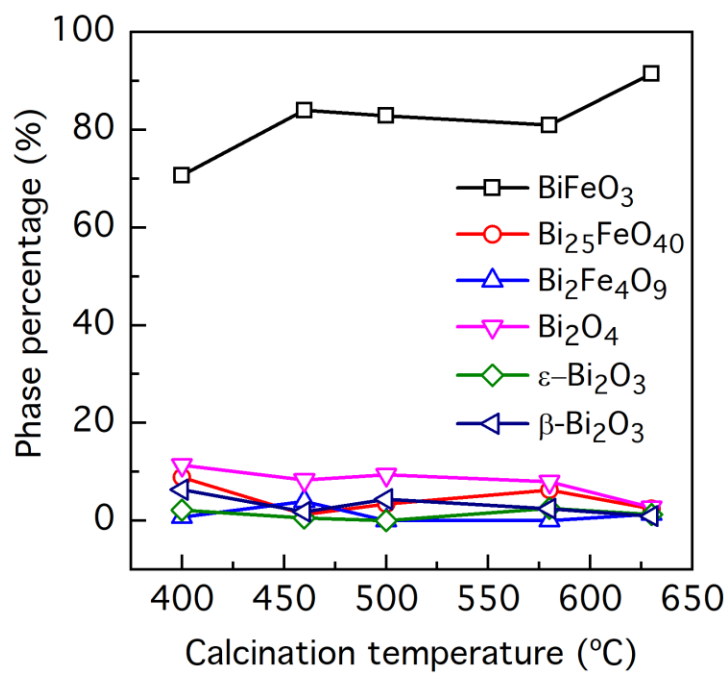


Figure S2. Phases employed in Rietveld refinement and its variation with the calcination temperature according to Rietveld refinements.

Table S1. Parameters obtained from Rietveld refinements for BiFeO₃ phase.

| | 400 °C | 460 °C | 500 °C | 580 °C | 630 °C |
|------------|---------|---------|---------|---------|---------|
| χ^2 | 2.9 | 9.9 | 5.3 | 6.4 | 2.4 |
| a, b (Å) | 5.5585 | 5.5804 | 5.5834 | 5.5807 | 5.5810 |
| c (Å) | 13.8764 | 13.8659 | 13.8780 | 13.8684 | 13.8750 |

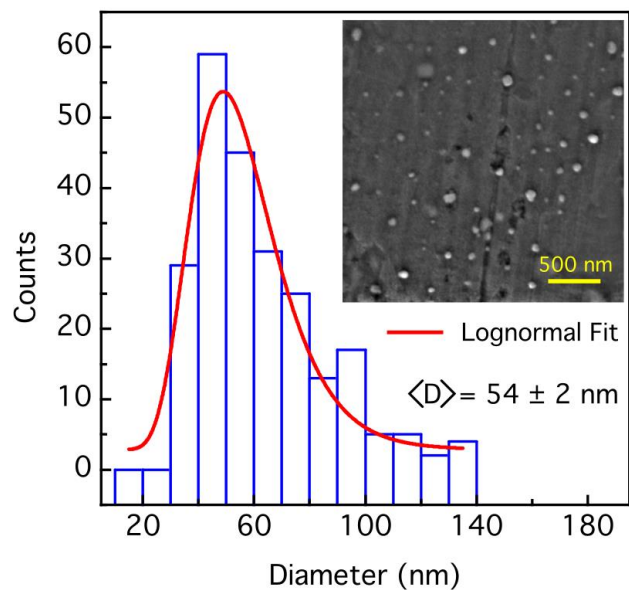


Figure S3. NPs size distribution obtained from FE-SEM images for NPs calcined at 630 °C. The lognormal fit is also shown. *Inset*: FE-SEM image for the named sample.

Table S2. Raman mode shifts for each sample calcined at different temperatures. Reference Raman mode positions for single crystal bulk BFO have been included for comparisons.

| Raman mode | Our study (cm ⁻¹) | | | | | Bulk BFO ¹¹ (cm ⁻¹) |
|---------------------------|-------------------------------|--------|--------|--------|--------|--|
| | 400 °C | 460 °C | 500 °C | 580 °C | 630 °C | |
| <i>E</i> 1 | 71 | 71 | 70 | 71 | 72 | 77 |
| <i>E</i> 2 | 90 | 92 | 92 | 96 | 96 | 136 |
| <i>A</i> ₁ – 1 | 124 | 127 | 126 | 128 | 127 | 147 |
| <i>A</i> ₁ – 2 | 161 | 162 | 162 | 164 | 164 | 176 |
| <i>A</i> ₁ – 3 | 209 | 209 | 209 | 210 | 212 | 227 |
| <i>E</i> 3 | 256 | 258 | 258 | 261 | 261 | 265 |
| <i>E</i> 4 | 299 | 301 | 299 | 306 | 304 | 279 |
| <i>E</i> 5 | 347 | 347 | 347 | 348 | 347 | 351 |
| <i>E</i> 6 | --- | --- | --- | --- | --- | 375 |
| <i>A</i> ₁ – 4 | 409 | 412 | 415 | 419 | 423 | 490 |
| <i>E</i> 7 | 467 | 467 | 466 | 466 | 467 | 437 |
| <i>E</i> 8 | 519 | 522 | 519 | 519 | 520 | 473 |
| <i>E</i> 9 | 628 | 629 | 621 | 622 | --- | 525 |

Table S3. Best fitting results obtained from the M vs H curves (taken at 300 K and 5 K) for each sample calcined at the temperature indicated. Fittings were performed using modified Langevin function and assuming a lognormal-like distribution of magnetic moments²⁶. N corresponds to the number of particles per unit mass and $\langle m \rangle$ to the average magnetic moment per particle. We also include a c parameter which is linear with the magnetic field and can be associated with the paramagnetic contribution to the NPs magnetization.

| $T_{\text{cal}} (^{\circ}\text{C})$ | 300 K | | | 5 K | | |
|-------------------------------------|--|-----------------------------|--|--|-----------------------------|--|
| | $N \left(\frac{1}{\text{kg}} \right)$ | $\langle m \rangle (\mu_B)$ | $c \left(\frac{\text{emu}}{\text{g}\cdot\text{Oe}} \right)$ | $N \left(\frac{1}{\text{kg}} \right)$ | $\langle m \rangle (\mu_B)$ | $c \left(\frac{\text{emu}}{\text{g}\cdot\text{Oe}} \right)$ |
| 400 | 4.8×10^{18} | 48 | 2.6×10^{-5} | 4.8×10^{18} | 50 | 1.6×10^{-5} |
| 460 | 4.3×10^{18} | 54 | 3.4×10^{-5} | 4.3×10^{18} | 58 | 2.6×10^{-5} |
| 500 | 9.2×10^{17} | 56 | 9.6×10^{-6} | 9.2×10^{17} | 59 | 1.5×10^{-5} |
| 580 | 1.8×10^{17} | 64 | 5.8×10^{-6} | 1.8×10^{17} | 68 | 1.5×10^{-5} |
| 630 | 1.2×10^{17} | 61 | 6.8×10^{-6} | 1.2×10^{17} | 70 | 3.2×10^{-5} |